Enriched End-member of Primitive MORB Melts: Petrology and Geochemistry of Glasses from Macquarie Island (SW Pacific)

VADIM S. KAMENETSKY[1]*, JOHN L. EVERARD[2], ANTHONY J. CRAWFORD[1], RICK VARNE[1], STEPHEN M. EGGINS[3,4] AND RUTH LANYON[1,4]

[1]SCHOOL OF EARTH SCIENCES AND CENTRE FOR ORE DEPOSIT RESEARCH, UNIVERSITY OF TASMANIA, GPO BOX 252-79, HOBART, TAS. 7001, AUSTRALIA

[2]TASMANIAN GEOLOGICAL SURVEY, PO BOX 56, ROSNY PARK, TAS. 7018, AUSTRALIA

[3]DEPARTMENT OF GEOLOGY, THE AUSTRALIAN NATIONAL UNIVERSITY, CANBERRA, A.C.T. 0200, AUSTRALIA

[4]RESEARCH SCHOOL OF EARTH SCIENCES, THE AUSTRALIAN NATIONAL UNIVERSITY, CANBERRA, A.C.T. 0200, AUSTRALIA

Macquarie Island is an exposure above sea-level of part of the crest of the Macquarie Ridge. The ridge marks the Australia–Pacific plate boundary south of New Zealand, where the plate boundary has evolved progressively since Eocene times from an oceanic spreading system into a system of long transform faults linked by short spreading segments, and currently into a right-lateral strike-slip plate boundary. The rocks of Macquarie Island were formed during spreading at this plate boundary in Miocene times, and include intrusive rocks (mantle and cumulate peridotites, gabbros, sheeted dolerite dyke complexes), volcanic rocks (N- to E-MORB pillow lavas, picrites, breccias, hyaloclastites), and associated sediments. A set of Macquarie Island basaltic glasses has been analysed by electron microprobe for major elements, S, Cl and F; by Fourier transform infrared spectroscopy for H_2O; by laser ablation–inductively coupled plasma mass spectrometry for trace elements; and by secondary ion mass spectrometry for Sr, Nd and Pb isotopes. An outstanding compositional feature of the data set (47·4–51·1 wt % SiO_2, 5·65–8·75 wt % MgO) is the broad range of K_2O (0·1–1·8 wt %) and the strong positive covariation of K_2O with other incompatible minor and trace elements (e.g. TiO_2 0·97–2·1%; Na_2O 2·4–4·3%; P_2O_5 0·08–0·7%; H_2O 0·25–1·5%; La 4·3–46·6 ppm). The extent of enrichment in incompatible elements in glasses correlates positively with isotopic ratios of Sr ($^{87}Sr/^{86}Sr = 0·70255–0·70275$) and Pb ($^{206}Pb/^{204}Pb = 18·951–19·493;$ $^{207}Pb/^{204}Pb = 15·528–15·589;$ $^{208}Pb/^{204}Pb = 38·523–38·979$), and negatively with Nd ($^{143}Nd/^{144}Nd = 0·51310–0·51304$). Macquarie Island basaltic glasses are divided into two compositional groups according to their mg-number–K_2O relationships. Near-primitive basaltic glasses (Group I) have the highest mg-number (63–69), and high Al_2O_3 and CaO contents at a given K_2O content, and carry microphenocrysts of primitive olivine ($Fo_{86-89·5}$). Their bulk compositions are used to calculate primary melt compositions in equilibrium with the most magnesian Macquarie Island olivines ($Fo_{90·5}$). Fractionated, Group II, basaltic glasses are saturated with olivine + plagioclase ± clinopyroxene, and have lower mg-number (57–67), and relatively low Al_2O_3 and CaO contents. Group I glasses define a seriate variation within the compositional spectrum of MORB, and extend the compositional range from N-MORB compositions to enriched compositions that represent a new primitive enriched MORB end-member. Compared with N-MORB, this new end-member is characterized by relatively low contents of MgO, FeO, SiO_2 and CaO, coupled with high contents of Al_2O_3, TiO_2, Na_2O, P_2O_5, K_2O and incompatible trace elements, and has the most radiogenic Sr and Pb regional isotope composition. These unusual melt compositions could have been generated by low-degree partial melting of an enriched mantle peridotite source, and were erupted without significant mixing with common N-MORB magmas. The mantle in the Macquarie Island

*Corresponding author. Fax: +61-3-62232547.
E-mail: Dima.Kamenetsky@utas.edu.au

region must have been enriched and heterogeneous on a very fine scale. We suggest that the mantle enrichment implicated in this study is more likely to be a regional signature that is shared by the Balleny Islands magmatism than directly related to the hypothetical Balleny plume itself.

INTRODUCTION

Geochemically enriched types of mid-ocean ridge basalts (MORB), variously referred to as transitional (T-), plume (P-) or enriched (E-) type MORB, contrast with the more abundant normal N-type MORB in having elevated concentrations of K_2O and other highly incompatible elements. These geochemically 'anomalous' MORB types occur either within distinct areas of ridge axis magmatism [e.g. FAMOUS and AMAR valleys, 14–16°N, 43°N of Mid-Atlantic Ridge (MAR), Oceanographer fracture zone, 12–13°N, 18–19°S, the Siqueiros fracture zone of the East Pacific Rise (EPR), Galapagos spreading centre, Southern Explorer Ridge, 7°E and 12–15°E of the SW Indian Ridge, Australian–Antarctic Discordance (Langmuir *et al.*, 1977; Shibata *et al.*, 1979; Schilling *et al.*, 1982, 1983; le Roex *et al.*, 1983, 1992; Bougault *et al.*, 1988; Hekinian *et al.*, 1989; Michael *et al.*, 1989; Natland, 1989; Klein *et al.*, 1991; Frey *et al.*, 1993; Niu *et al.*, 1996, 1999)] or compose off-axis seamounts randomly distributed within oceanic plates in the vicinity of spreading centres (Batiza & Vanko, 1984; Zindler *et al.*, 1984; Allan *et al.*, 1994; Niu & Batiza, 1997). Their formation is commonly attributed to the influence of near-ridge plumes or hotspots, or alternatively to the presence of heterogeneities (blobs or veins of enriched material) in a depleted peridotite mantle.

Inhomogeneities of unknown size, composition and origin in the mantle source region are usually invoked to explain the correlation between trace element and radiogenic isotope characteristics reported in many MORB suites [so-called 'coupled MORB' of Niu *et al.* (1996)]. Alternatively, MORB suites with limited isotopic variations but more extensive incompatible element ratio variations have been attributed to mixing of primary melts formed by different extents of melting of an isotopically homogeneous source [e.g. FAMOUS (Langmuir *et al.*, 1977; Frey *et al.*, 1993); EPR at 21°N (Dupre *et al.*, 1981; Macdougall & Lugmair, 1986)]. Another type of chemical 'coupling' between major elements (e.g. MgO) and incompatible trace element ratios was also recorded for some MORB lavas (e.g. Frey *et al.*, 1993; Allan *et al.*, 1994; Niu *et al.*, 1999) and interpreted in terms of two-component mixing (Niu *et al.*, 1999), although this phenomenon has not yet been fully evaluated.

If erupted MORB were primary or near-primary magmas, it might be possible to use the coupling between major and trace element contents and isotopic ratios to distinguish the potential roles in MORB magma genesis of source heterogeneities vs partial melting of a homogeneous source. However, popular notions of melt generation, segregation and extraction (e.g. McKenzie & Bickle, 1988; Natland, 1989) predict that discrete primary melts are extremely rare or even absent in the oceanic lithosphere. Rather, it has been suggested that the generally uniform erupted N-MORB magmas are produced by extensive polybaric mixing and fractionation of diverse melt fractions formed within a melting column. Therefore, source heterogeneities and the extents of mantle melting processes are generally obscured within the relatively long-lived and robust magmatic systems located beneath oceanic spreading centres. Recent studies of melt inclusions trapped within MORB phenocrysts of primitive composition have added to our knowledge of the geochemistry of primary melts with identification of contrasting ultra-depleted to ultra-enriched trace element compositions (e.g. Sobolev & Shimizu, 1993, 1994; Shimizu, 1994; Kamenetsky, 1996; Tsamerian & Sobolev, 1996; Kamenetsky & Crawford, 1998; Kamenetsky *et al.*, 1998). However, the post-entrapment crystallization and re-equilibration of melt inclusions, combined with our current inability to perform radiogenic isotope analyses on individual melt inclusions, place significant limitations on any reconstruction of the major element and isotopic compositions of primary melts.

In this paper we present the results of petrological and geochemical studies of hyaloclastites and pillow-rim glasses sampled from Macquarie Island, an exposure above sea-level of the Macquarie Ridge system. The results indicate that some of the glasses represent primitive, near-primary melts, which span a large geochemical range from N-MORB to highly enriched varieties. The fact that their major element, radiogenic isotope and trace element geochemical characteristics are all well correlated represents a new contribution to the continuing debate on the nature of MORB primary and parental melts, source heterogeneity, parameters and effects of melting.

TECTONIC SETTING OF MACQUARIE ISLAND

Macquarie Island (54°30′S, 158°56′E) and a few nearby islets constitute the only exposure above sea-level of the Macquarie Ridge, an elongate arcuate bathymetric high mostly lying at <2000 m water depth, which extends for 1200 km SSW from New Zealand (47°S) to about 57°S
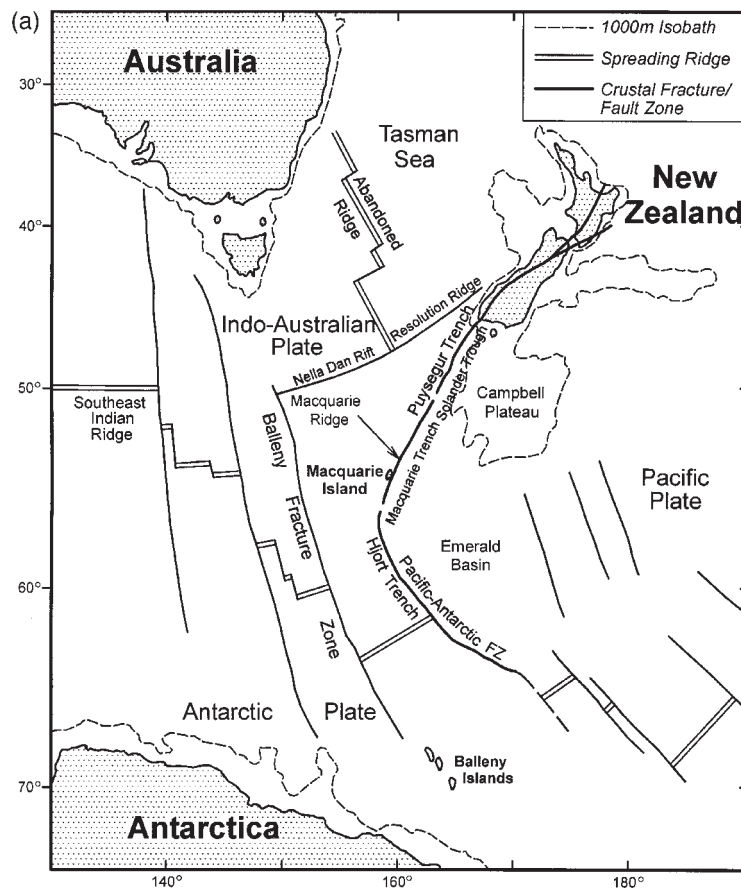
Fig. 1. (a) Map of South Pacific–Southern Ocean region showing location of the Macquarie Ridge and Macquarie Island.

(Fig. 1a). Rocks dredged from the Macquarie Ridge include tholeiitic MORB-like basalt, dolerite, olivine gabbro, troctolite and serpentinized harzburgite (Watkins & Gunn, 1971; Ovenshine *et al.*, 1974; Schilling & Ridley, 1974; Matveyenkov & Baranov, 1981; Mortimer, 1995) and resemble those from Macquarie Island.

The Macquarie Ridge, together with an adjacent and parallel trench system, marks the boundary between the Australia and Pacific plates, and was formed from ocean crust in the last 10 My by transcurrent to compressional relative motion (transpression) resulting from a mismatch in the rates of Australia–Antarctic and Pacific–Antarctic sea-floor spreading (Johnson & Molnar, 1972; Ruff *et al.*, 1989).

The ridge is seismically very active [average return period 1 year for magnitude >6·2, magnitude 7·8 recorded in 1943 (Jones & McCue, 1988)]. The seismicity is shallow and probably limited to the crust (Ruff *et al.*, 1989), indicating that subduction is not occurring at present. Earthquake fault plane solutions for the Macquarie segment suggest sub-horizontal, east–west oriented principal stress axes, and probably dextral strike-slip

movement along fault planes parallel to the ridge (Jones & McCue, 1988). This implies counter-clockwise rotation of the Pacific plate, relative to the Australian plate, and right lateral strike-slip movement along the Macquarie Ridge.

The ridge is divided into four discrete segments (Hayes & Talwani, 1972; Massell *et al.*, 2000) by marked breaks in its continuity and strike near 51°S, 53°S and 56°S. Along the Macquarie segment (53°S to 56°S, including the Macquarie Island region), the shallow depth and flat-topped morphology of the ridge suggest that much of the Macquarie segment might have been at sea-level in the past (Griffin & Varne, 1980; Massell *et al.*, 2000). The ridge is here paralleled by the Macquarie Trench, which lies immediately to its east, mostly at 5000–6000 m water depth.

Gravity studies suggest that about 400 km NNE of Macquarie Island the ocean crust of the Australian plate thickens from ∼7 km, west of the Macquarie Ridge, to 14 km just east of the ridge (Williamson & Johnson, 1974). This is consistent with 65 km of crustal shortening by transpression (Williamson, 1988).
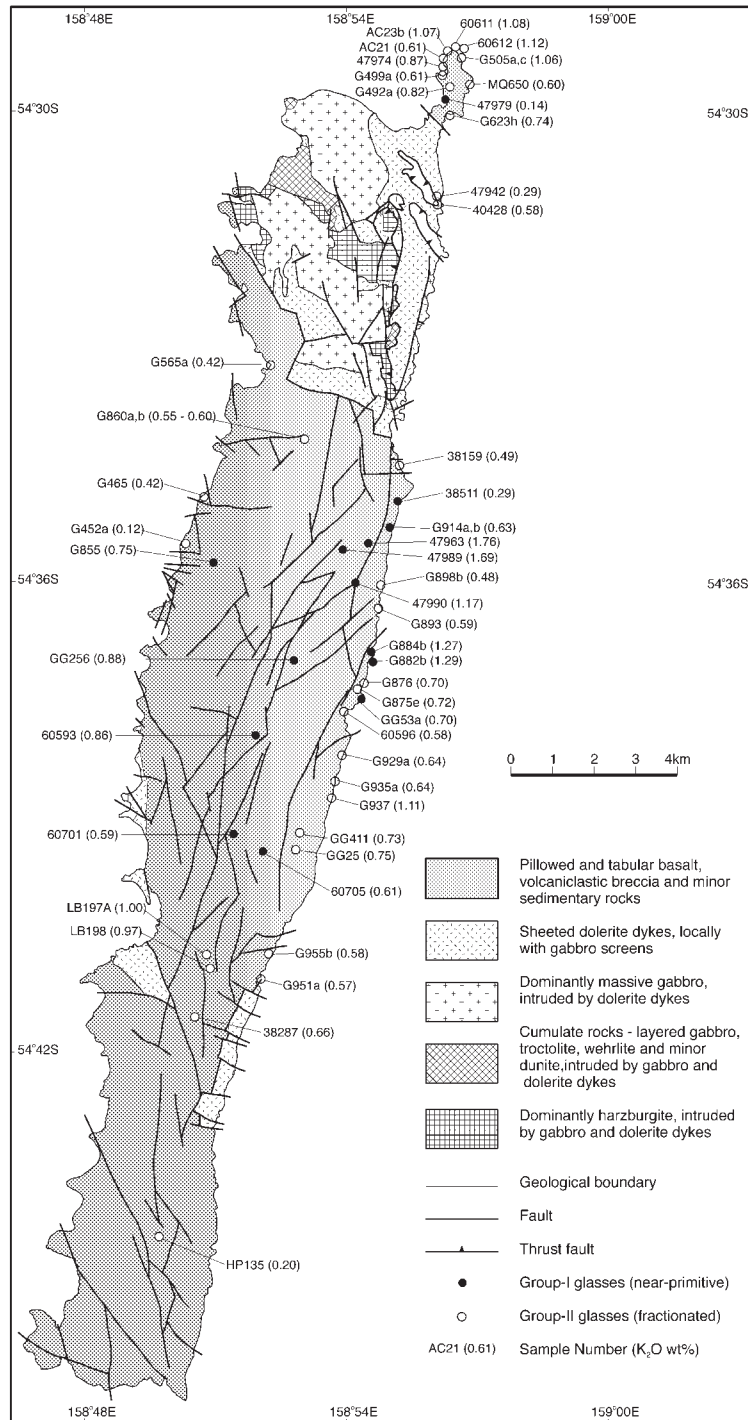
Fig. 1. (b) Geological map of Macquarie Island and locations of glass samples.

West of the Macquarie segment, the crust of the South Tasman Basin slopes gently down to ∼4000 m. This crust belongs to the Australia plate, and between the Balleny Fracture Zone to the west and the southern part of the Macquarie Ridge to the east (Fig. 1a), is assigned to the Balleny spreading corridor (Cande *et al.*, 1998)

formed by spreading at the Southeast Indian Ridge that began in Cretaceous times, and has continued until the present. To the east, between the ridge and the continental Campbell Plateau margin (Fig. 1), lies the Emerald Basin ($\sim$4000 m), on the Pacific plate.

The magnetic anomaly system of the Balleny spreading corridor has been traced northwards to the east-trending bathymetric features of the Nella Dan rift and its eastern continuation, the Resolution Ridge system (Cande *et al.*, 1998). The location of these bathymetric structures corresponds to the angular magnetic unconformity between the magnetic anomalies of the Tasman Sea and the younger anomalies of the oceanic crust of the Balleny spreading corridor, generated at the Southeast Indian Ridge. The now extinct Tasman spreading centre (Fig. 1a) can be easily identified on gravity anomaly maps [see fig. 2 of Sutherland (1995)].

Weissel *et al.* (1977) identified magnetic anomaly 7 (25 Ma) to the west of Macquarie Island, and Williamson (1988) argued that this anomaly was traceable eastward, across Macquarie Island to the Macquarie Trench. This would imply that the ocean crust exposed on Macquarie Island was formed at the Southeast Indian Ridge by late Oligocene spreading, and remains part of the Australia plate, and that the Macquarie Trench marks the plate boundary.

However, in the vicinity of Macquarie Island, the Macquarie Ridge has a double crest with a central valley, and the island is an exposure of the eastern ridge crest (Summerhayes, 1969; Massell *et al.*, 2000). According to Massell *et al.* (2000), the active transcurrent plate boundary in the Macquarie segment coincides with a zone of multiple ridge-parallel lineaments confined to the central valley, rather than with the Macquarie Trench, as Williamson (1988) supposed. Macquarie Island is therefore now located on the Pacific plate.

Moreover, new gravity and swath data acquired for the oceanic crust south of New Zealand support a new explanation for the tectonic evolution of the region in general and for the Macquarie Island region in particular.

The Resolution Ridge and the western margin of the Campbell Plateau plus the eastern boundary of the Emerald Basin (Fig. 1a) are conjugate margins, formed in Eocene times by the rifting of continental and older oceanic crust when the Australia–Pacific boundary developed into a spreading ridge south of New Zealand (Sutherland, 1995).

Fracture zones and tectonic spreading fabric within this triangle of new oceanic crust record the evolution since Eocene times of the Australia–Pacific boundary from a spreading system into a system of long transform faults linked by short spreading segments, and now into a right lateral strike-slip plate boundary (Sutherland, 1995; Wood *et al.*, 1996; Lamarche *et al.*, 1997; Massell

et al., 2000). Plate reconstruction models show the Australia–Pacific relative pole of rotation migrating southeast, away from the New Zealand landmass, during late Eocene–late Miocene times, and remaining close to the plate boundary south of New Zealand, its closeness implying slow spreading at the plate boundary. It then migrated southwest, even nearer the plate boundary, during Plio-Pleistocene time (Walcott, 1978; Stock & Molnar, 1982; Sutherland, 1995).

Lamarche *et al.* (1997) estimated that spreading and oceanic crust creation may have continued at the Australia–Pacific plate boundary immediately south of New Zealand until 12–16 My ago, and their model for the evolution of the plate boundary geometry shows it still active as a spreading plate boundary in the Macquarie Island region at 11 Ma (their fig. 6C).

Varne *et al.* (2000) have used the new swath data of Massell *et al.* (2000) for the Macquarie Island region, coupled with data from Deep Sea Drilling Project (DSDP) Site 278, magnetic anomaly data of Weissel *et al.* (1977) in the Emerald Basin, and calculated spreading rates of Lamarche *et al.* (1997) for conjugate crust, to calculate that oceanic crust of the Macquarie Island region was still being created 9–14 My ago at the Australia–Pacific plate boundary. This is in agreement with radiometric and palaeontological ages for rocks of the island (see the next section).

REGIONAL GEOLOGY OF MACQUARIE ISLAND

Macquarie Island, $\sim$37 km long and between 3 and 5 km wide (Fig. 1b), is elongate in a NNE direction along the Macquarie Ridge. In most parts a narrow shore platform rises steeply to a plateau $\sim$250–300 m above sea-level, with a maximum elevation of 433 m. Dating of raised beach deposits on the plateau suggests an uplift rate of $\sim$0·8 mm/year, implying that the island has been emergent for only 0·6–0·7 My (Adamson *et al.*, 1996). Seismic activity and the presence of numerous active fault scarps indicate continuing tectonism.

The earliest geological work on Macquarie Island, by L. R. Blake (1911–1914), was published by Mawson (1943), but the island was first recognized as an uplifted fragment of ocean crust by Varne *et al.* (1969). Subsequent work includes that of Varne & Rubenach (1972), Griffin & Varne (1980), Griffin (1982), Christodoulou *et al.* (1984), Lees (1987), Duncan & Varne (1988) and Varne (1989), and the island has recently been systematically mapped at 1:10 000 scale by the Tasmanian Geological Survey (Goscombe & Everard, 1998, 1999).

Faulting, on all scales with a spacing down to a few metres, pervades the island (Fig. 1b). The greatest tectonic uplift has occurred in the northern quarter of the island,

exhuming a tilted middle- to lower-crustal section of sheeted dolerite dykes, which pass downward with increasing frequency of gabbro screens to massive gabbro and then into a cumulate sequence of layered olivine gabbro, troctolite, minor plagioclase wehrlite, wehrlite and dunite and finally to residual mantle harzburgite (Griffin & Varne, 1980; Basylev & Kamenetsky, 1998). This section is everywhere disrupted by numerous faults (although reasonably continuous along the northwestern coast), and gabbros, cumulates and harzburgites are all intruded by dolerite dykes. Fault-bounded blocks and thrust slices of extrusives (mostly pillow basalt) are also present, most notably at the northeastern extremity of the island.

The southern three-quarters of the island (Fig. 1b) consists mainly of basaltic pillow lavas with subordinate massive to tabular basalt flows, hyaloclastite, rare picrite and minor pelagic sedimentary rocks (mostly red mudstone, with rare sandstone and conglomerate). The basalts are highly porphyritic (>50% plagioclase $\pm$ olivine $\pm$ clinopyroxene) to aphyric and include some rare hornblende-bearing types. Calcareous oozes occur between pillows, and are widely distributed although not abundant.

The extrusive sequence is intensely faulted. Narrow basaltic dykes that cut the extrusive rocks were intruded at a high angle to bedding. The volcanic rocks were first tilted around axes that were near-horizontal and parallel to dyke–bedding plane intersections, causing variations in dip, and later rotated about vertical axes, causing variations in strike (Varne & Rubenach, 1972). Palaeomagnetic data (Williamson, 1979) suggest that clockwise rotation of kilometre-sized fault blocks has occurred.

An uplifted fault block composed of sheeted dolerite dykes, with rare gabbro screens, occurs along the southeast coast. An occurrence of sheeted dolerite dykes along the central west coast lacks gabbro screens and in places passes, both laterally and upward, into extrusive sequences.

There is general agreement that Macquarie Island is built of rocks that were formed at an oceanic spreading centre (Varne et al., 1969; Varne & Rubenach, 1972; Griffin & Varne, 1980; Christodoulou et al., 1984; Goscombe & Everard, 1998, 1999; Varne et al., 2000) but the timing and location of the spreading was disputed. From the central third of the island, a massive basalt flow has yielded a well-defined $^{40}Ar/^{39}Ar$ plateau age of $11·5 \pm 0·3$ Ma, and a hornblende separate from a massive flow or near-surface intrusion yielded a K–Ar age of $11·5 \pm 0·3$ Ma, both interpreted as original crystallization ages (Duncan & Varne, 1988). A basalt from the northernmost headland of the island (Fig. 1b) yielded a well-defined $^{40}Ar/^{39}Ar$ plateau age of $9·7 \pm 0·3$ Ma, which Duncan & Varne (1988) again interpreted

as its original crystallization age. Nearby, poorly preserved coccoliths from oozes associated with pillow lavas were thought by Quilty et al. (1973) to be of early or middle Miocene age (11–24 Ma), and Foraminifera from oozes suggest a late Miocene (5–11 Ma) or younger age (Varne et al., 1969). The radiometric and palaeontological ages are therefore broadly in keeping with the range of 9–14 Ma for the timing of the generation of oceanic crust in the Macquarie Island region independently calculated by modelling of the tectonic history (Varne et al., 2000).

PETROGRAPHY AND MINERALOGY

Glasses occur both as quenched rims of basaltic pillow lavas and, more commonly, as fragments in hyaloclastite breccias. The latter usually consist of subangular to angular or rounded glass lapilli, glassy and crystalline pillow fragments, up to 3 cm ($\sim$40% of breccias), and may carry olivine and/or plagioclase crystals, in a matrix of smaller glassy debris cemented by a greenish grey aggregate possibly after shattered and dispersed glass. Carbonates, zeolites and smectite–chlorite intergrowths are commonly present in interstices and as tiny veins in the hyaloclastites. In thin section the glasses are transparent and dark to light brown in colour, and may contain scattered opaque devitrified zones rich in crystallites. Microphenocrysts of olivine (20–300 μm) with trapped spinel and glass inclusions are widespread but make up <5 vol. %. In some glasses octahedra of reddish brown spinel and laths of plagioclase are also present, although no clinopyroxene crystals were observed. Microphenocrysts of olivine and plagioclase are skeletal to euhedral and show no signs of resorption or textural disequilibrium.

Large vesicles filled with aggregates of secondary minerals and surrounded by alteration haloes are common within many of the glasses. Alteration seems to have begun along cooling contraction fractures in glasses, and expanded away from these, resulting in polygonal areas of fresh glass set in a matrix of alteration products.

ANALYTICAL METHODS

A total of 56 glasses from Macquarie Island and two glasses from Macquarie Ridge were crushed and fresh chips were hand-picked and analysed for major elements, S, Cl and F, using a Cameca SX50 electron microprobe (University of Tasmania) and basaltic glass VG-2 as an internal standard. Special care was taken to avoid altered areas within the glasses and the vicinity of microphenocrysts where compositional heterogeneities are more likely to occur. Each reported glass composition is the average of at least 15 analyses. Glasses have very

homogeneous compositions (low standard deviation values), and the analytical errors in determination of each of the major element oxides are as follows (in rel. %): 0·7–0·9 (SiO_2, Al_2O_3); 1·5–2·2 (FeO, MgO, CaO); 2·7–5 (TiO_2, Na_2O, K_2O); 12 (P_2O_5).

Fourier transform infrared (FTIR) spectroscopy measurements of H_2O in glasses were obtained using a Bruker IFS66 FTIR spectrometer at the University of Tasmania. Details of the technique and calibration have been given by Danyushevsky *et al.* (1993).

Trace elements in glasses were analysed by LA-ICPMS (laser ablation–inductively coupled plasma mass spectrometry) at the Research School of Earth Sciences, Australian National University, Canberra, using an ArF (193 nm) EXCIMER laser, a Fisons PQ2 STE ICPMS instrument, and custom-built sample introduction system (Eggins *et al.*, 1998). Analyses were performed using a spot size of 200 μm and a laser pulse rate of five repetitions per second. The total analysis time for each sample was 130 s, comprising a 60 s background and 70 s analysis with laser on. Sixty replicate measurements were made for each isotope. Standard glass NIST 612 was used for calibration. Data reduction was performed using background subtracted count rates and the methods outlined by Longerich *et al.* (1996). ^{43}Ca was employed as the internal standard isotope, based on CaO concentrations measured by electron probe. Analytical precision of the measurements is in the range 1–5% for most elements.

Isotope analyses of Sr, Nd and Pb in six glasses were performed at the Research School of Earth Sciences, Australian National University, Canberra, using a Finnigan MAT261 mass spectrometer operated in static multi-collector mode. Details of sample preparation and analytical technique have been reported by Lanyon (1994) and Woodhead (1996).

CHEMICAL COMPOSITION OF GLASSES
Major and trace element compositions

All the analysed Macquarie Island glasses are basaltic in composition, with 47·4–51·1 wt % SiO_2 and 5·65–8·75 wt % MgO (Table 1), and include both saturated (hypersthene-normative) and undersaturated (nepheline-normative) compositions in about equal proportions. An outstanding feature of the glasses is their large range of major element abundances, in particular K_2O (0·12–1·76 wt %), Na_2O (2·37–4·24 wt %) and TiO_2 (0·97–2·10 wt %), and moderately to highly incompatible element abundances [e.g. Rb (3·2–59·5 ppm), La (4·3–46·6 ppm), Eu (0·92–2·0 ppm)].

The glasses have been subdivided into two distinct compositional groups (Table 1, Fig. 2) using the relationship between their *mg*-number [Mg/(Mg + Fe^{2+}), where Fe^{2+} = 0·9Fe^{total}) and contents of highly incompatible elements. The latter are best expressed by K_2O/TiO_2 or La/Sm as these ratios are not strongly affected by crystal fractionation of ol + plag, which mostly increases the absolute abundances of incompatible elements. In the description and following discussion we use La/Sm as an index of degree of enrichment, though other ratios such as Rb/K, Zr/Ti or Nb/Zr could be used equally well. Eighteen Group I glasses have the highest *mg*-number (63·2–69·1) at a given K_2O content (K_2O/TiO_2, La/Sm) and their compositions form a regular trend with a negative slope in Fig. 2. Thirty-eight Group II glass compositions are scattered below this trend, and have relatively lower *mg*-number (57·1–67·2) at similar K_2O abundances.

Group I or near-primitive glasses, defined as having the highest *mg*-number (the lowest FeO at a given MgO), also have the highest Sr/Nd, Ba/Rb and Sc/Yb values at a given La/Sm value, as well as the lowest Zr/Sm and Hf/Eu and heavy rare earth element (HREE) and Y abundances (Fig. 3, Table 1). They also carry phenocrysts and microphenocrysts of relatively primitive olivine $Fo_{85·8–89·5}$ and Cr-spinel [mean *cr*-number, Cr/(Cr + Al), is 35].

In contrast, Group II or fractionated glasses carry more evolved olivine crystals in most samples ($Fo_{83·5–88·3}$), spinel grains with higher *cr*-number (mean 42), and plagioclase ($An_{76–88}$). Fractionation of olivine, plagioclase and clinopyroxene in the genesis of the Group II glasses is reflected in their lower *mg*-number Al, Ca, Sc, Sr and Ba, and higher SiO_2, FeO, Hf (Zr) and HREE abundances (Figs 2–4). It should be noted that the enriched members (La/Sm >7) of Group I glasses do not have counterparts among fractionated compositions.

Group I glasses show a seriate variation within the compositional spectrum of MORB, and extend the compositional range from N-MORB compositions to enriched compositions that seem to represent a new primitive enriched MORB end-member. Their range in MgO abundances from low (down to 5·9 wt %) to high (up to 8·8 wt %), found, respectively, in the most enriched and the least enriched Group I Macquarie glasses (Fig. 4), appears to be typical of many other E- to N-MORB suites (le Roex *et al.*, 1983, 1992; Batiza & Vanko, 1984; Bougault *et al.*, 1988; Allan *et al.*, 1993, 1994; Niu & Batiza, 1997; Niu *et al.*, 1999). Although the MgO contents of enriched Group I glasses are too low to allow the interpretation of these glasses as primary mantle-derived melts, they have strikingly low FeO contents (Table 1, Fig. 4). Indeed, addition of only 5–8% equilibrium olivine would bring these compositions into equilibrium with mantle olivine $Fo_{90·5}$ (see below). However, the Group I

Table 1: Representative major and trace element compositions of Macquarie Island glasses

	1	2	3	4	5	6	7	8	9	10	11	12	13
Sample:	47979	25637	G855	GG256	G882b	47963	G452a	HP135	38287	G492a	LB197a	25601	
SiO_2	49·56	49·30	48·31	48·05	47·94	48·18	49·96	50·58	49·74	49·65	49·44	49·16	44·70
TiO_2	0·97	1·19	1·38	1·46	1·61	1·91	1·35	1·72	2·10	1·63	1·82	1·75	2·76
Al_2O_3	17·09	17·25	17·77	18·03	17·96	18·17	15·49	15·03	15·97	17·27	17·28	17·52	14·34
FeO*	8·06	7·50	7·55	7·18	7·03	6·81	9·47	10·17	9·59	8·10	8·19	7·55	11·23
MnO	0·14	0·17	0·14	0·07	0·09	0·08	0·13	0·18	0·17	0·13	0·13	0·15	0·18
MgO	8·75	8·36	7·80	7·34	6·59	5·90	8·13	6·83	6·68	6·96	5·85	6·77	7·47
CaO	12·82	12·69	11·93	11·24	11·25	10·85	11·59	11·12	10·18	10·61	10·25	10·02	10·72
Na_2O	2·37	2·58	2·99	3·53	3·57	4·24	2·60	2·54	3·37	3·29	3·62	3·70	3·17
K_2O	0·14	0·42	0·75	0·88	1·29	1·76	0·12	0·20	0·66	0·82	1·00	1·10	1·31
P_2O_5	0·08	0·21	0·28	0·33	0·47	0·66	0·13	0·17	0·35	0·36	0·51	0·40	0·61
F	0·034	0·022	0·037	0·059	0·062	0·078	0·013	0·013	0·038	0·047	0·065	0·040	
S	0·076	0·082	0·083	0·075	0·073	0·078	0·104	0·112	0·107	0·081	0·087	0·075	
Cl	0·013	0·029	0·051	0·066	0·096	0·140	0·010	0·015	0·047	0·059	0·088	0·079	
H_2O	0·25	0·52	0·78	n.d.	1·30	1·49	0·30	0·45	0·88	0·84	n.d.	1·13	2·41†
mg-no.	68·3	68·8	67·2	67·0	65·0	63·2	63·0	57·1	58·0	63·0	58·6	64·0	
Cs	0·047	0·115	0·253	0·307	0·516	0·654	n.d.	0·051	0·245	0·273	0·372	0·402	
Be	0·407	0·481	0·735	0·877	1·155	1·542	0·366	0·584	0·977	0·980	1·196	1·229	
B	0·703	1·46	1·73	1·71	3·49	2·56	0·942	1·82	2·39	2·23	2·19	2·68	
Sc	33·6	32·1	29·6	27·3	27·3	24·2	35·5	38·3	31·7	28·7	26·7	26·8	
Ti	6174	7258	8822	9324	10425	11913	8455	10405	13062	10471	11026	11003	
V	210	220	205	192	186	178	283	317	299	217	212	210	
Ga	16·2	15·6	16·5	16·2	16·2	17·8	17·6	18·4	20·1	18·6	18·4	19·6	
Rb	3·63	13·3	24·5	30·9	44·9	59·5	3·24	6·07	22·0	26·7	34·7	36·7	
Sr	155	246	335	397	555	703	111	141	225	367	402	443	
Y	18·8	20·3	21·9	23·0	22·3	22·6	27·1	35·0	38·9	26·0	28·1	24·9	
Zr	54·9	77·1	90·1	109	130	163	72·4	110	160	131	148	146	
Nb	7·16	24·5	43·7	54·4	69·6	91·4	5·94	10·6	39·0	40·8	52·6	53·5	
Ba	38·6	134	242	303	444	584	31·3	53·7	190	249	317	337	
La	4·62	13·3	21·6	26·4	35·8	46·6	4·33	7·55	21·0	22·4	28·4	28·7	
Ce	11·3	27·1	41·7	51·1	66·4	86·3	12·2	19·1	44·1	44·2	54·7	56·5	
Nd	7·57	13·3	17·8	20·9	26·9	33·0	9·53	13·6	23·1	20·5	24·5	23·9	
Sm	2·26	3·12	3·72	4·19	5·04	5·93	3·10	4·11	5·69	4·59	5·20	4·89	
Eu	0·925	1·14	1·35	1·52	1·73	2·01	1·20	1·50	1·89	1·60	1·78	1·72	
Gd	2·84	3·43	3·87	4·22	4·58	5·12	3·99	5·24	6·33	4·67	5·22	4·79	
Dy	3·40	3·69	3·91	4·20	4·20	4·39	4·80	6·24	6·98	4·75	5·22	4·72	
Er	2·06	2·28	2·32	2·43	2·29	2·35	2·92	3·86	4·22	2·77	2·93	2·64	
Yb	1·98	2·11	2·23	2·39	2·16	2·13	2·92	3·70	4·03	2·55	2·75	2·47	
Lu	0·290	0·319	0·339	0·352	0·320	0·306	0·433	0·553	0·602	0·367	0·410	0·366	
Hf	1·47	1·98	2·30	2·73	3·12	3·66	2·15	3·04	3·98	3·18	3·63	3·50	
Ta	0·418	1·40	2·45	3·09	3·88	5·08	0·338	0·641	2·27	2·33	3·06	3·03	
Pb	0·503	0·971	1·39	1·69	2·22	2·89	0·504	0·709	1·43	1·58	1·93	2·02	
Th	0·494	1·83	3·18	4·06	5·26	7·04	0·427	0·833	2·92	3·22	4·28	4·21	
U	0·155	0·484	0·855	1·13	1·39	1·94	0·127	0·225	0·779	0·909	1·13	1·24	

1–6, Group I 'near-primitive' glasses; 7–12, Group II 'fractionated' glasses; 13, average composition of the Balleny plume lavas with MgO = 6–8 wt % (Lanyon, 1994). All oxides in wt %; trace elements in ppm. *mg*-no. = $Mg/(Mg + Fe^{2+})$ in mol %, where $Fe^{2+} = 0.9FeO$. n.d., not determined. The complete set of glass compositions is available from the senior author upon request.
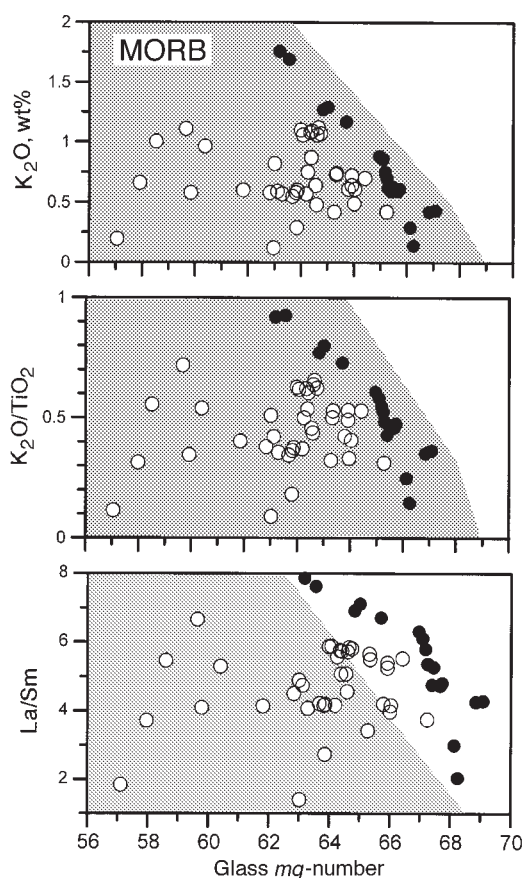*All Fe as FeO.
†Loss on ignition.

Fig. 2. Relationships between *mg*-number and incompatible elements (K_2O) and their ratios (K_2O/TiO_2 and La/Sm) in Macquarie Island Group I (●) and Group II (○) glasses. Field of MORB glasses comprises numerous data sources and our unpublished data. It should be noted that Group I compositions are arbitrarily defined as having the highest *mg*-number at a given degree of enrichment, and they are among the most primitive MORB compositions.

glasses are still among the least fractionated MORB melts known, because this correction for olivine fractionation is relatively small and because neither plagioclase nor clinopyroxene were on their liquidus (Figs 3 and 4).

Significant variations in incompatible major, trace and volatile element concentrations and ratios are observed in both Group I and II glasses (Figs 2–5). Particularly apparent is the wide range in concentration of the most incompatible trace elements (Fig. 5; Table 1: e.g. Rb/Yb 1·1–27·9, La/Yb 1·5–21·9). Although the degree of enrichment in many Group I glasses is exceptional, even for E-MORB, it is, however, similar to that observed in many alkali ocean island basalts (OIB). In particular, it bears strong similarities to the regional OIB from Balleny and Scott islands (Fig. 5a). The geochemical patterns of Macquarie Island glasses on PM- (primitive mantle) normalized diagrams (Fig. 5) share the following features of the regional OIB signature: a negative K anomaly,

greater abundances of Ta and Nb relative to the adjacent incompatible trace elements, and a general decrease in the abundances of elements more incompatible than Ta and Nb. These features, which are characteristic of HIMU ocean island basalts (Weaver, 1991; Woodhead, 1996), have also been reported from many E-MORB suites (Langmuir *et al.*, 1977; Wood, 1979; le Roex *et al.*, 1983, 1992; Bougault *et al.*, 1988; Niu & Batiza, 1997). The most significant difference, however, is the more pronounced depletion of HREE in the OIB relatively to even the most enriched Macquarie Island MORB glasses.

The glasses appear to have preserved magmatic compositions remarkably well, as suggested by the excellent correlation of all incompatible elements (Fig. 5). This phenomenon extends to low abundance and/or highly mobile elements (e.g. Cs, Be, Fig. 6), not usually analysed for, and even to volatile elements. For example, H_2O (0·25–1·49 wt %) and Cl (0·01–0·14 wt %) contents are positively correlated with other highly incompatible elements and the degree of enrichment (Fig. 6). There is a tendency for H_2O and Cl to be slightly higher in the Group II compared with the Group I glasses, which is a likely result of crystal fractionation.

Glass isotope compositions

Radiogenic isotope data for four Group I and two Group II Macquarie glasses are presented in Table 2 and Fig. 7. Sr, Nd and Pb isotope values for these glasses correlate well with their major and trace element compositions (Fig. 7b): enriched glasses have the most radiogenic Pb and Sr ratios.

The isotopic compositions of the studied glasses show a much greater affinity with Pacific MORB than with Indian Ocean MORB, particularly in their generally higher $^{206}Pb/^{204}Pb$ values (Fig. 7a). Their isotopic compositions indicate the presence of a distinctive regional mantle isotopic signature characterized by high Nd and low Sr isotopic ratios, similar to MORB, and high $^{206}Pb/^{204}Pb$ values intermediate between those of MORB and HIMU OIB and indicative of time-integrated elevated U/Pb. Although the isotopic compositions of the Macquarie glasses generally overlap with Pacific MORB, particularly in Pb–Pb space, they trend towards a HIMU-like isotopic component similar to the Balleny plume (Fig. 7a, and Hart, 1988; Lanyon *et al.*, 1993; Lanyon, 1994).

Olivine–glass relationships and primary melt compositions

The presence of olivine phenocrysts and microphenocrysts in the Macquarie Island glasses suggests that at least some of the olivine grains have crystallized from the liquid that transported them to the surface and then
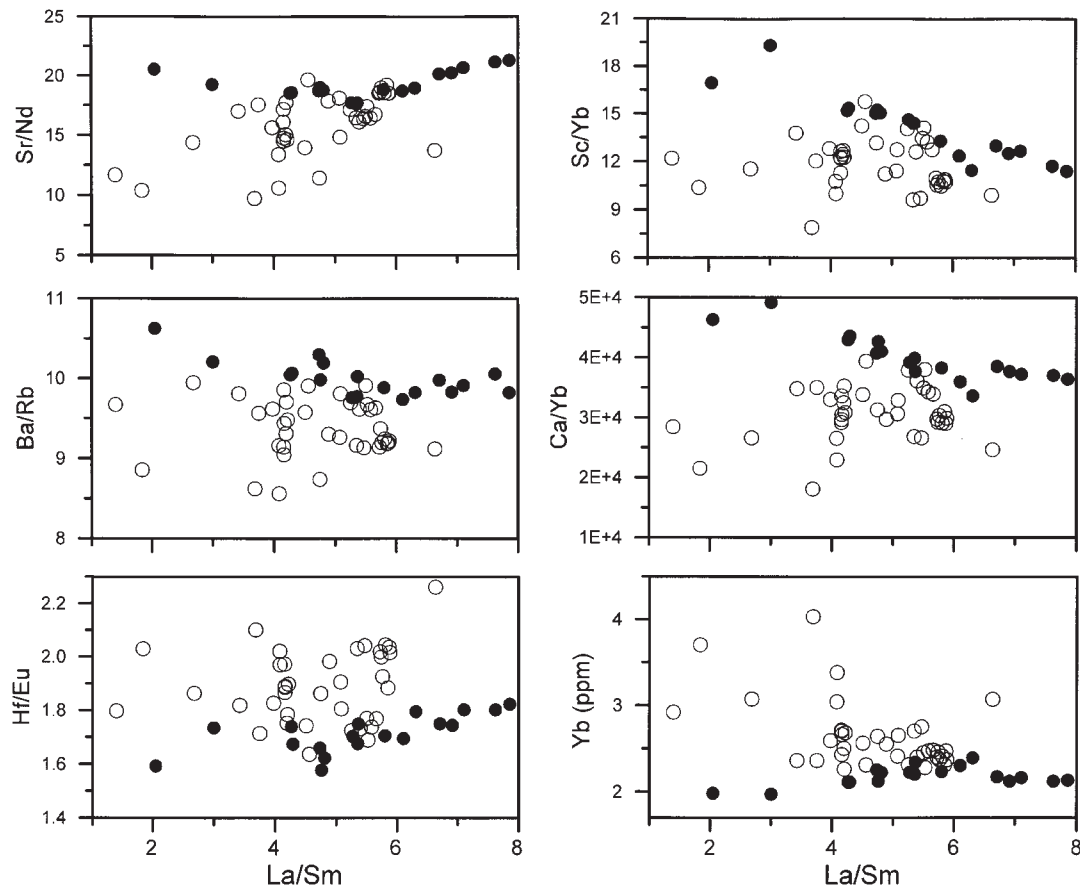
Fig. 3. Relationships between La/Sm and Yb and ratios of trace elements (Sr/Nd, Ba/Rb, Hf/Eu, Sc/Yb, Ca/Yb) similarly incompatible during partial mantle melting (Sun & McDonough, 1989) in the Macquarie Island glasses. Symbols as in Fig. 2. It should be noted that Group II glass compositions are affected by plagioclase (lower Sr/Nd and Ba/Rb and higher Hf/Eu) and clinopyroxene (lower Sc/Yb and Ca/Yb) fractionation.

quenched to form a glass. However, the possibility that some or all of the olivine crystals are xenocrysts should also be considered. The genetic relationship between the olivine crystals and their host glass can be investigated using the compositions of melt inclusions trapped in olivine, and calculated olivine–melt equilibria.

Most olivine crystals within glasses contain melt inclusions (up to 100 μm), which represent small portions of melt trapped during crystallization. Optically, melt inclusions have the appearance of glass, and their composition is depleted in MgO (Table 3) and enriched in all other elements. These features are explained by the post-entrapment crystallization of olivine onto the walls of the inclusions. However, the ratios of elements that are incompatible in olivine (e.g. K_2O/TiO_2, Na_2O/TiO_2, CaO/Al_2O_3) remain unaltered. Comparison of these incompatible element ratios in melt inclusions with their values in the host glass (Table 3) shows that olivine phenocrysts crystallized from a liquid identical to the host glass in terms of incompatible element ratios.

A comparison of olivine compositions with the calculated compositions of olivine in equilibrium with their host glasses is shown in Fig. 8. The most evolved (Fe-rich) crystals in each sample are in equilibrium with the host glass, as is indicated by $K_{dOl-melt}^{Mg-Fe^{2+}} = 0.27–0.30$. The presence of more Fo-rich olivines, whose compositions are not in equilibrium with their host glasses, suggests their crystallization from more primitive magmas. This implies that none of the Macquarie Island glasses can represent a primary melt in terms of *mg*-number. The most primitive olivine compositions found in the Group I glasses range from $Fo_{88.2}$ in high-K glasses to $Fo_{89.5}$ in low-K glasses. These olivine Fo values match closely the compositions of the most primitive olivines found in the Macquarie Island low-K picrites ($Fo_{90.5}$), cumulate peridotites ($Fo_{90.5}$) and restite peridotites ($Fo_{91.5}$) (Basylev & Kamenetsky, 1998), and also abyssal mantle peridotites worldwide (Fo_{91}, Dick, 1989). Therefore, the compositions of the most Fo-rich olivine within the Macquarie glasses can be used in association with the Group I glass
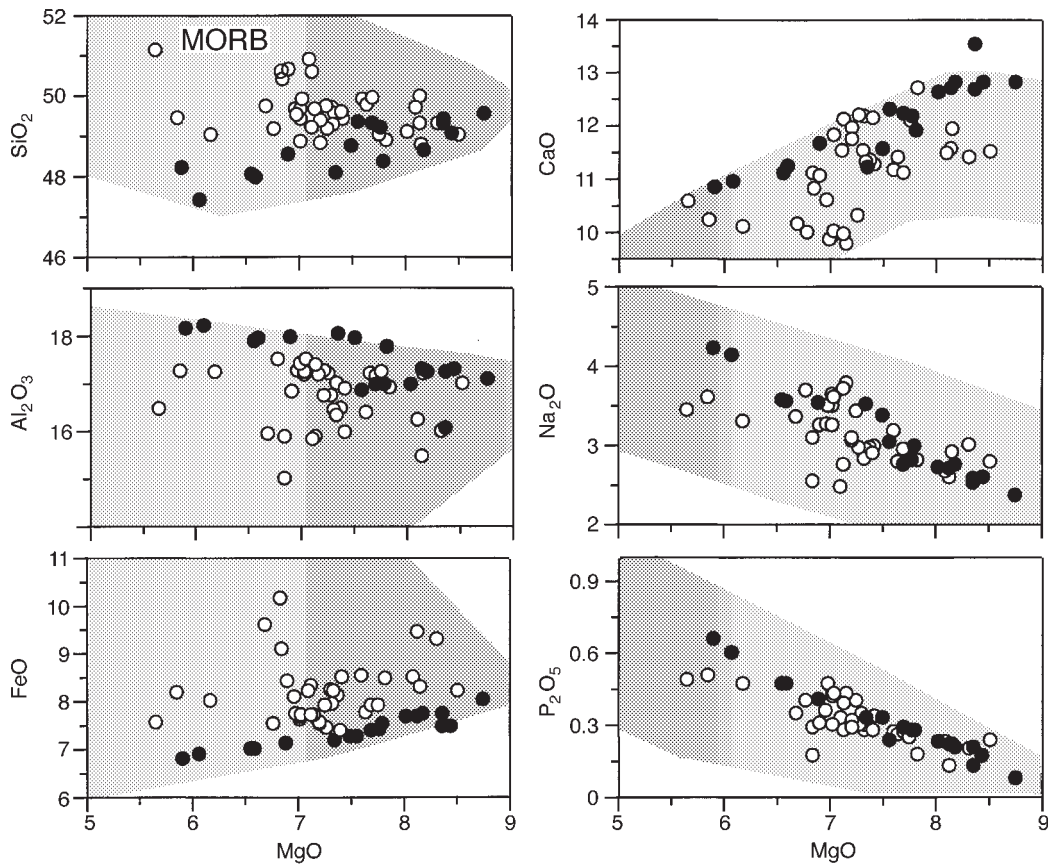
Fig. 4. Major element composition of the Macquarie Island glasses in comparison with MORB glass field (numerous data sources and our unpublished data). Symbols as in Fig. 2; oxides in wt %. The effect of plagioclase and possibly clinopyroxene crystallization on the composition of Group II glasses is evident from reduced Al_2O_3 and CaO abundances. It should be noted that Group I glass compositions border the least fractionated MORB compositions on MgO vs SiO_2, Al_2O_3, FeO and CaO plots.

compositions to estimate the composition of near-primary melt with which the olivine would be in equilibrium.

To calculate the compositions of Macquarie Island near-primary melts from the compositions of Group I glasses we assumed that the effects of spinel and plagioclase (where they are present in glasses) crystallization were insignificant. The measured compositions of the Group I glasses were corrected for olivine-only crystallization by adding olivine component in the amount required to maintain an olivine–melt equilibrium (Ford *et al.*, 1983) until calculated equilibrium with the most primitive Macquarie Island olivine ($Fo_{90.5}$) was achieved. The degree of iron oxidation in melts ($Fe^{2+}/Fe^{3+} = 6.7$) was calculated using the mean Fe^{2+}/Fe^{3+} of Cr-spinel and the empirical model for spinel–melt equilibria (Maurel & Maurel, 1982). The results obtained for representative Group I glasses from calculating their 'primary' melt compositions and crystallization temperatures are presented in Table 4. The amount of added olivine does

not exceed 5–8 wt %, and it could be even smaller, and thus MgO of primary melts could be lower, if we overestimated the Fo content of liquidus olivine in the enriched primary magmas and it is less than $Fo_{90.5}$.

This discussion tacitly assumes that the compositions of glasses as measured by electron probe represent the bulk compositions of the erupted melts. However, the glasses carry microphenocrysts of olivine that apparently crystallized, at least in part, where they are now found. Therefore, the analysed glass compositions do not represent original melt compositions because these have been modified by olivine extraction. The olivine microphenocrysts make up 5 vol. % (equivalent to ~6 wt %) or less of the samples. This amount is roughly similar to the amount of olivine added during the correction procedure (~5–8 wt %). It is possible, therefore, that the actual magma compositions fell between the analysed glass compositions and the calculated 'primary' melt compositions of Table 4.
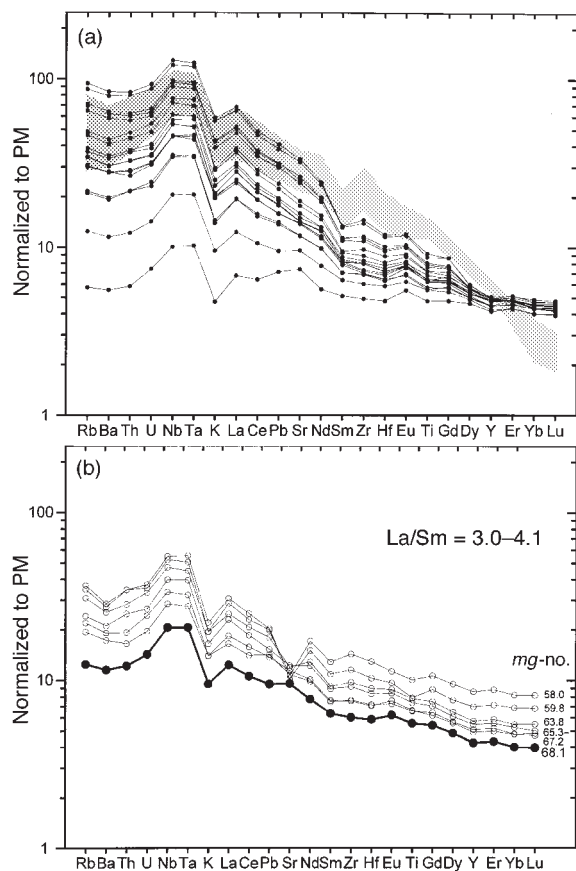
Fig. 5. Primitive mantle-normalized (Sun & McDonough, 1989) trace element patterns for (a) Group I glasses compared with the field of plume-related lavas from Balleny Province (Lanyon, 1994). The broad range of variations in the most incompatible elements and relative constancy of abundances of elements more compatible than Dy should be noted; (b) Group II fractionated glasses with La/Sm = 3·0–4·1 and *mg*-number = 67·2–58·0 compared with Group I glass 38511 (La/Sm = 3·0, *mg*-number = 68·1), which can be considered as their parental melt.

Fig. 6. La/Sm vs highly mobile (Cs, Be) and volatile (Cl, H_2O) elements. Symbols as in Fig. 2.

DISCUSSION

Evidence for a primitive enriched member in the MORB family

The major and trace element diversity demonstrated by the Macquarie Island glasses has allowed two compositional groups to be distinguished. These near-primitive (Group I) and fractionated (Group II) melts are genetically related via the process of olivine ± plagioclase ± clinopyroxene crystallization. To a certain extent, the geochemical dispersion recognized in the primitive Group I glasses has been inherited by the more evolved Group II glasses, although the most enriched compositional varieties (La/Sm >7) are found exclusively among Group I glasses. Taking into account the large number of samples studied, it is therefore tempting to assign genetic
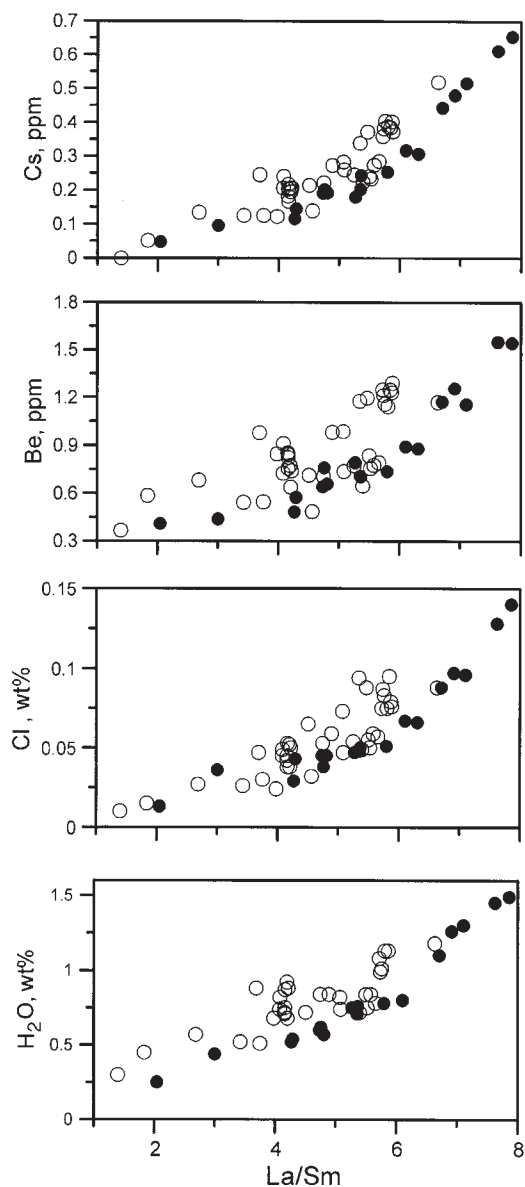
significance to the fact that the enriched primitive compositions lack counterparts amongst the fractionated glasses. However, this can be readily explained by the fact that the elevated H_2O contents of enriched melts up to 1·5 wt % (Table 1, Fig. 6) cause a significant delay in plagioclase crystallization (Housh & Luhr, 1991). In addition, the original enriched magmas were probably erupted without suffering extensive mixing and fractionation, probably as a result of their being the first melt fractions within an immature magmatic system, i.e. before a magma chamber(s) developed. This is generally consistent with the observations that the sites of ephemeral

Table 2: Strontium, Nd and Pb isotope data for Macquarie Island glasses

Sample:	47979	25637	78	47963	38287	25601
$^{87}Sr/^{86}Sr$	0·702551	0·702614	0·703315*	0·702743	0·702636	0·702748
$^{143}Nd/^{144}Nd$	0·513100	0·513095	0·513040	0·513050	0·513071	0·513061
$^{206}Pb/^{204}Pb$	18·951	19·384	19·41	19·493	19·275	19·294
$^{207}Pb/^{204}Pb$	15·528	15·562	15·574	15·589	15·559	15·565
$^{208}Pb/^{204}Pb$	38·523	38·876	38·927	38·979	38·828	38·808
MgO wt %	8·75	8·36	6·24	5·90	6·68	6·77
La/Sm	2·05	4·27	6·27	7·86	3·69	5·87

Major and trace element compositions are given in Table 1 (except sample 78).
*We consider this ratio to be shifted from the initial magmatic value as a result of seawater alteration.

to minor E-MORB magmatism coincide with the settings of off-axis seamounts (Batiza & Vanko, 1984; Zindler *et al.*, 1984; Allan *et al.*, 1994; Niu & Batiza, 1997), extremely slow spreading ridges above regions of diffuse mantle upwelling (le Roex *et al.*, 1992), or tectonically complex regions that are transitional between transform faults and ridge systems, along which diffuse, locally concentrated extension is occurring (Allan *et al.*, 1993).

Alkali-enriched lavas associated with typical depleted MORB are being increasingly frequently reported (e.g. le Roex *et al.*, 1983, 1992; Batiza & Vanko, 1984; Bougault *et al.*, 1988; Allan *et al.*, 1993, 1994; Niu & Batiza, 1997), and the Macquarie Island enriched glass compositions have many features in common with other E-MORB suites, including their HIMU affinities. However, the Macquarie Island Group I glasses are unique in that they have:

(1) the greatest enrichment in K_2O and highly incompatible trace elements (Figs 2 and 5a), Al_2O_3 and CaO (Fig. 4), and depletion in SiO_2 and FeO (Fig. 4) at a given *mg*-number (MgO);

(2) the most primitive (near-primary) compositions, modified by olivine crystallization only, at a given degree of enrichment (Figs 2 and 8);

(3) strong bivariate correlations between major, trace and volatile element abundances and isotope ratios (Figs 2–7);

(4) a well-defined compositional transition from enriched compositions to compositions typical of low-K MORB (Figs 2 and 4).

Despite the general similarity in incompatible trace element compositions between enriched Macquarie glasses and HIMU oceanic intraplate basalts, and regional Balleny plume lavas in particular (Fig. 5a), notable striking differences in key major element and HREE contents (Table 1, Fig. 5a) and discrepancy in isotope composition (Fig. 7a) between the enriched Macquarie Island MORB and Balleny plume OIB make it difficult to assign the

magmatism to an OIB mantle source. In other words, Macquarie Island melts are not the melting products of Balleny plume. Moreover, the presence of sheeted dykes, the relatively low calculated temperatures of primary Macquarie Island magmas (Table 4) and typical MORB values of spinel *cr*-number (26–56, compared with >54 in OIB spinel) are in disagreement with the idea of hotspot oceanic magmatism. Therefore, we argue that the magma type represented by Macquarie Island Group I enriched glasses defines a new primitive end-member within the known compositional spectrum of MORB. It is characterized by the lowest abundances of MgO, FeO, SiO_2 and CaO coupled with the highest concentrations of Al_2O_3, TiO_2, Na_2O, P_2O_5, K_2O and incompatible trace elements, and has the most radiogenic Sr and $^{206}Pb/^{204}Pb$ regional isotope composition.

This is not to disregard the possibility that the upper-mantle source might have intermixed with material from the Balleny plume. An important tectonic feature of the region is a postulated mantle plume trace, extending southward from eastern Tasmania ($\sim$40–45 Ma) and marked by a chain of seamounts, passing west of the Macquarie Ridge, and ending in the active volcanoes of the Balleny Islands north of the Ross Sea (Lanyon *et al.*, 1993). Magmas resulting from this plume activity differ from typical ocean floor basalts in having a HIMU-like signature (Fig. 7a) and OIB major and trace element compositions (Table 1, Fig. 5a).

Primitive glass trends: mixing vs melting

Group I primitive glasses show remarkably well correlated variations in the concentrations of the major, trace and volatile elements and their ratios (Figs 2–6). The consistent seriate compositional trends from the enriched compositions to those typical of N-MORB argue for a certain linkage in the genesis of these diverse compositions. Two mechanisms, namely melt mixing and
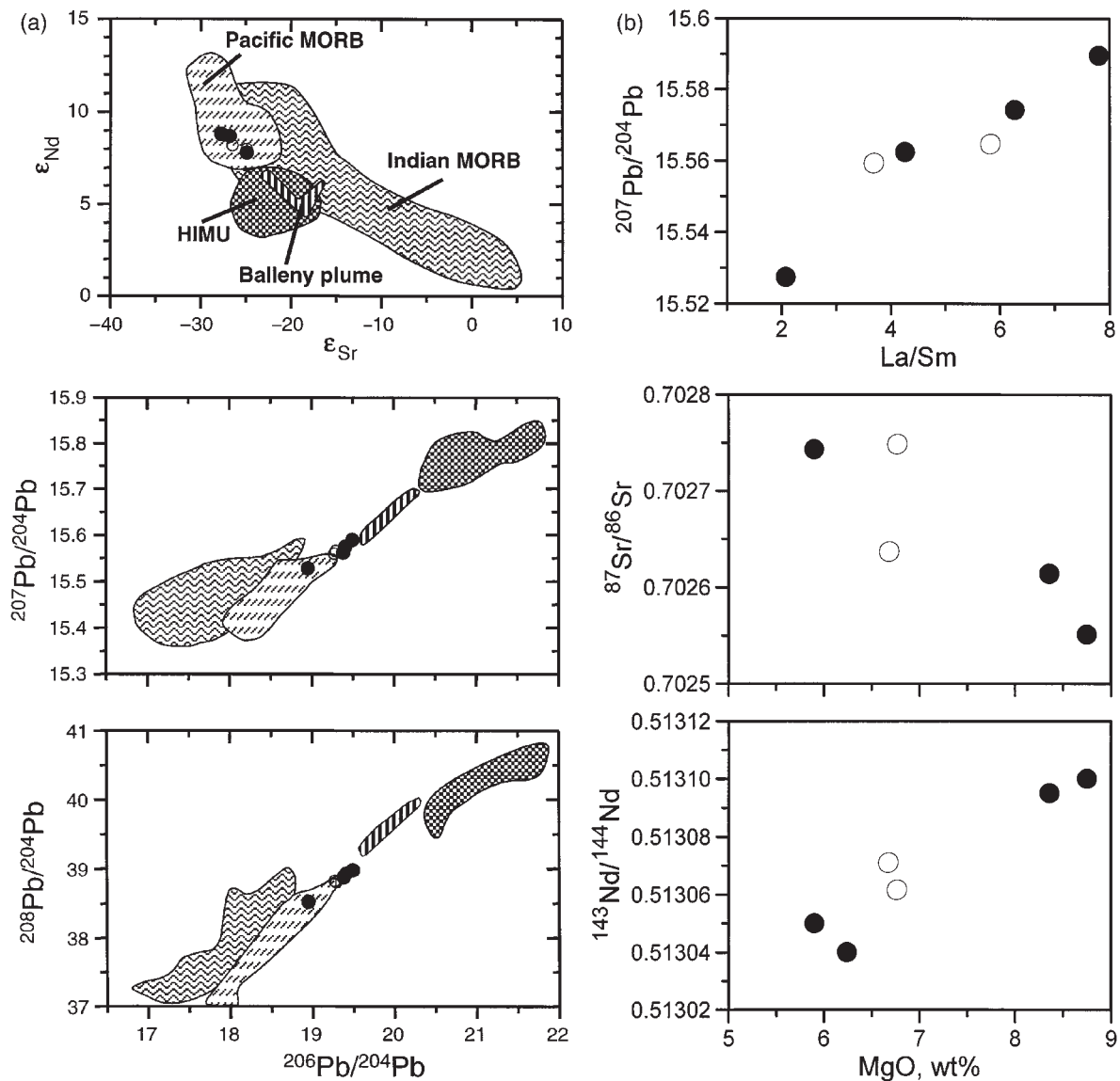
Fig. 7. Correlation between isotope, major and trace element compositions of Macquarie Island glasses. Symbols as in Fig. 2. Also shown are fields for Pacific and Indian Ocean MORB and HIMU basalt (numerous data sources) and Balleny province rocks (Lanyon, 1994).

fractional melting, might account for the observed co-variations.

Mixing between enriched and depleted 'end-member' melts, generated from different mantle lithologies or even within different source regions, is the most simple explanation for the linear covariations of elements of similar incompatibility. However, the binary mixing of the two geochemical 'end-members' defined by our data is inconsistent with the trends observed (Figs 3 and 9). On the other hand, multistage mixing or contamination of an initial dominant volume of enriched melt with very minor and nearly constant amounts of a depleted end-member component could produce non-linear geochemical trends with little dispersion along them. In both variants of mixing the presence of a depleted melt in the mantle at all stages of melting or in the magmatic system is essential. This is a keystone of the so-called 'melting-induced two-component mixing' model (Niu *et al.*, 1996; Niu & Batiza, 1997), which requires the melting of highly depleted mantle to be triggered by an interaction with, and solidus temperature reduction by, highly enriched melts. As enriched melts cannot be generated from the same depleted mantle source, a heterogeneous mantle becomes a vital component of the above model.

Dynamic (critical, continuous or near-fractional) partial melting, during which both pressure and source composition change (Langmuir *et al.*, 1977; Maaloe, 1982; Eggins, 1992), produces virtually the same trends of melt

Table 3: Comparison between the compositions of glassy inclusions in olivine and host glass

Sample:	47963		25603	
	Melt inclusions	Glass	Melt inclusions	Glass
n:	17		39	
K_2O/TiO_2	0.90 ± 0.06	0.92	0.61 ± 0.04	0.60
CaO/Al_2O_3	0.62 ± 0.03	0.60	0.59 ± 0.03	0.58
Na_2O/TiO_2	2.18 ± 0.11	2.22	2.01 ± 0.12	2.01
TiO_2/Al_2O_3	0.101 ± 0.004	0.105	0.099 ± 0.005	0.105
MgO, wt %	2.79–5.79	5.90	3.92–7.76	7.02
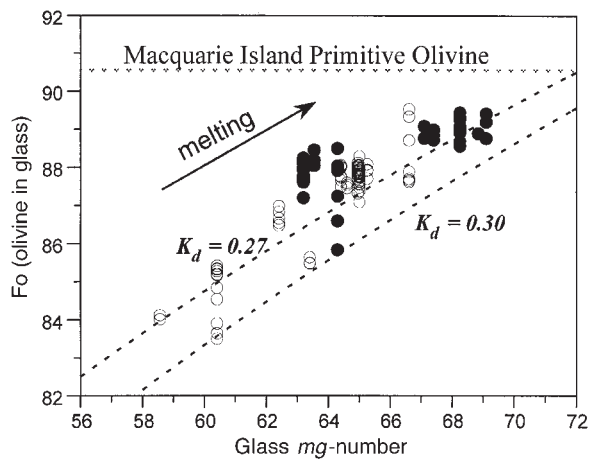
Fig. 8. Forsterite content of the olivines plotted against *mg*-number of their host glasses showing that the most evolved olivine crystals in each sample are in equilibrium with the host glasses. K_d is the coefficient of distribution of Mg–Fe^{2+} between olivine and melt. Symbols as in Fig. 2.

Table 4: Representative compositions of Macquarie Island primary melts in equilibrium with olivine Fo$_{90.5}$ calculated using Group I glass compositions

Sample:	47979	25637	G855	GG256	G882b	47963
SiO_2	48.87	48.74	47.73	47.52	47.31	47.51
TiO_2	0.9	1.12	1.28	1.36	1.48	1.75
Al_2O_3	15.85	16.23	16.52	16.83	16.51	16.67
Fe_2O_3	1.19	1.1	1.12	1.07	1.06	1.03
FeO	7.15	6.66	6.74	6.43	6.38	6.22
MnO	0.13	0.16	0.13	0.07	0.08	0.07
MgO	11.59	10.71	10.63	10.05	9.91	9.34
CaO	11.89	11.94	11.09	10.49	10.34	9.95
Na_2O	2.2	2.43	2.78	3.29	3.28	3.89
K_2O	0.13	0.4	0.7	0.82	1.19	1.61
P_2O_5	0.07	0.2	0.26	0.31	0.43	0.61
Tol, °C*	1287	1270	1275	1267	1266	1272
% Olivine†	7.1	5.8	6.9	6.6	8	8.1

The compositions of Macquarie Island Group I (near-primitive) glasses that have been used to calculate primary melts are given in Table 1. Calculations were performed using program PETROLOG.
*Temperature of olivine–melt 'dry' equilibrium calculated using Ford *et al.* (1983) model.
†Total wt % of added olivine to achieve melt equilibrium with Fo$_{90.5}$, the most primitive olivine found in Macquarie Island rocks.

composition as does fractional melting of a heterogeneous mantle followed by melt mixing and accumulation (Natland, 1989). According to Langmuir *et al.* (1977), variations in trace element abundances and their ratios can result from different degrees of partial melting of a rising mantle source that is undergoing continuous but incomplete removal of melt as melting proceeds. In an extension of this model, Plank & Langmuir (1992) suggested that a homogeneous mantle source can produce magmas that are mixtures of numerous instantaneous melt fractions produced at various points throughout the melting regime. This interpretation can be successfully applied to the primitive Macquarie glasses, although in this case the integration of discrete melt packets either had a minimal effect or did not occur at all.

The major element systematics of the Group I Macquarie glasses are consistent with continuous variations in the extent of melting, as defined by the global major element systematics of MORB (Klein & Langmuir, 1987; Langmuir *et al.*, 1992) and isobaric experimental batch melts (e.g. Jaques & Green, 1980; Fujii & Scarfe, 1985; Kinzler & Grove, 1992a, 1992b). For example, if the La/Sm value is taken as a measure of the extent of melting (F), then for Macquarie Island the transition from low- to higher-F melts is characterized by increasing SiO_2, FeO, MgO and CaO, and decreasing TiO_2, Al_2O_3, Na_2O, K_2O and P_2O_5 (Figs 2 and 4, Table 4). Using the Macquarie Island data, the 'seemingly fortuitous relationship between incompatible element enrichment and MgO' (Plank & Langmuir, 1992) and between radiogenic isotopes and MgO (Fig. 7b) could be accounted for by positive correlation between the degree of melting and the MgO content of the partial melts. The fact that the Group I glasses retain their original major and trace element signatures also implies that melts may become mobile and segregate from their mantle source regions at very small volume percent, and their rapid migration towards the surface (probably via channel flow) can prevent re-equilibration at lower pressures.
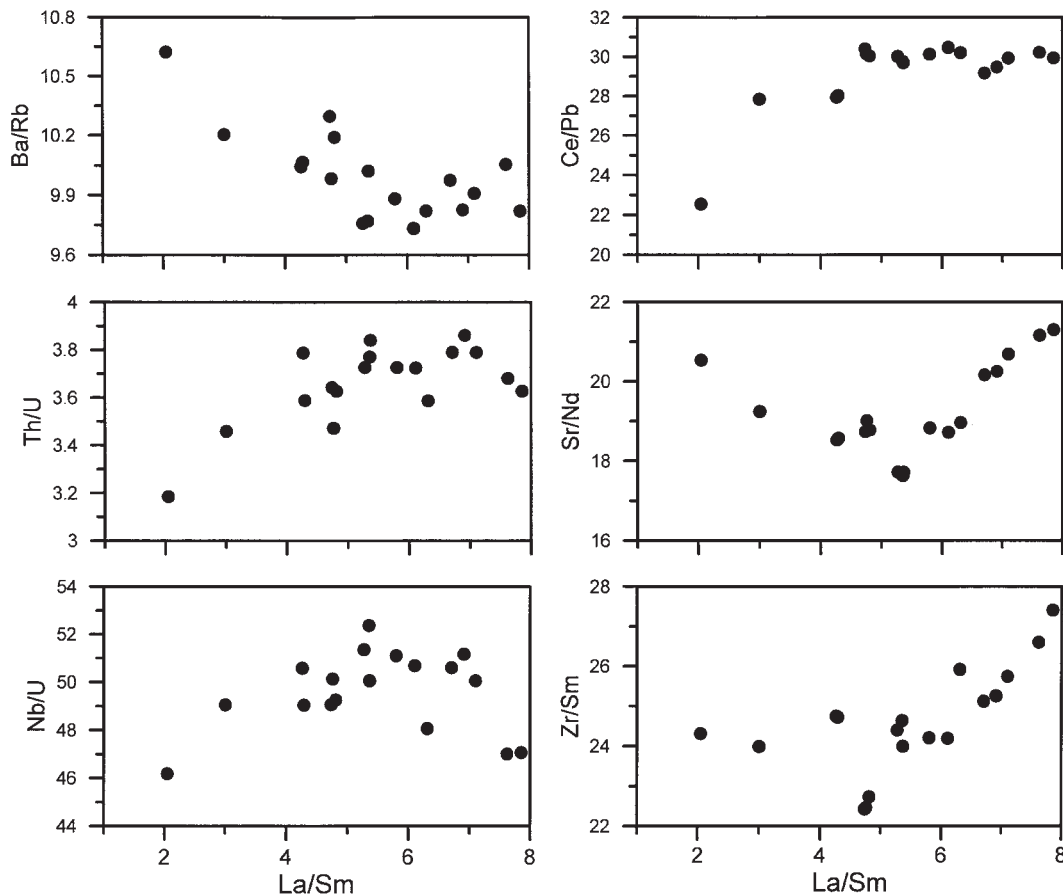
Fig. 9. La/Sm vs ratios of trace elements similarly incompatible during partial mantle melting (Sun & McDonough, 1989) in Macquarie Island Group I glasses. The change in elements' incompatibility at different La/Sm should be noted.

Plank & Langmuir (1992) explained the local trends and global variations of fractionation-corrected Na_2O and Ce abundances in MORB as resulting from end-member mixing between high-degree and low-degree melts derived from a homogeneous depleted source (Fig. 10). In this diagram the Group I Macquarie glasses form a steep trend which extends from the so-called 'melting baseline' (Plank & Langmuir, 1992) towards a composition moderately enriched in Na_2O and highly enriched in Ce. This extreme enrichment in Ce and other highly incompatible elements (e.g. by a factor of ∼20 in terms of Rb) cannot be explained even invoking the lowest possible extents of melting (<1%) of depleted mantle (Ce 0·7 ppm, Plank & Langmuir, 1992). Therefore, a source that was originally more enriched than N-MORB but progressively depleting as a result of melting

towards the composition of a typical N-MORB source can be suggested for Macquarie Island melts.

A role for mantle heterogeneities in the origin of primary melts

The radiogenic isotope diversity of MORB is usually ascribed to chemical and isotopic heterogeneities in the mantle. These heterogeneities are thought to be represented by enriched material, which in many cases is interpreted to originate by partial melting of complex mantle including deep mantle plume-derived enriched mantle and enriched upper-mantle asthenosphere. The range of Pb isotope compositions in Macquarie Island glasses as well as the range of incompatible elements are
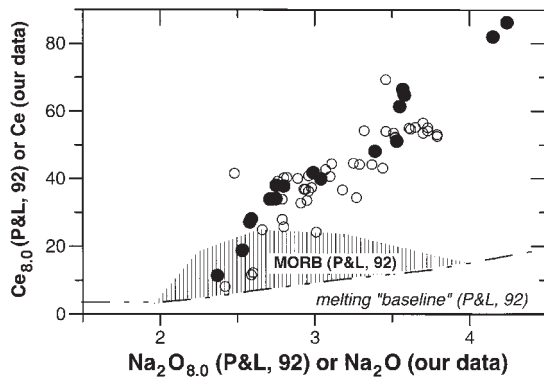
Fig. 10. Na_2O vs Ce compositions of the Macquarie Island glasses compared with the MORB field and 'melting baseline' of Plank & Langmuir (1992). The steep trend of glass compositions implies melting of LREE-enriched source. Symbols as in Fig. 2.

therefore suggestive of geochemical heterogeneities in the mantle source region. The scale of mantle heterogeneities must be very small to account for distinct compositions of lavas within such a small area as Macquarie Island. However, this simple model cannot explain all of the compositional features of Macquarie Island melts and requires further development.

The rate of re-equilibration of isotopic and chemical heterogeneities with the rest of the mantle is a function of many factors [see review by Zindler & Hart (1986)], most of which are hard to determine quantitatively. The most important factors are the size of the heterogeneity and cation diffusion rates. The latter depend on mantle phase composition, diffusion direction, temperature, and the presence or absence of fluid or melt phases in the system. Small-scale heterogeneities may survive re-equilibration and thus be represented in partial melts either in fluid- or melt-free mantle over a long time period, or if they were introduced into the mantle just before melting. In the latter case, the melting can be readily attributed to formation of enriched mantle domains.

Correlations between isotopes, and major and incompatible trace element characteristics in the Macquarie Island glasses (Fig. 7b) imply not only that these chemical factors are coupled in the source, but that the elements and isotope ratios fractionate synchronously during melting. This, combined with the improbability of a simple two end-member melt mixing, supports a conclusion that the mantle source was homogeneous on a large scale, but heterogeneous on a very small, probably grain-size, scale. From observations of changes in the relative incompatibility of elements that usually do not fractionate from each other over short intervals of melting (Fig. 9), we conclude that the mineral assemblage of the mantle source also experienced melting-related modifications. The most pronounced changes in geochemical behaviour of certain elements (e.g. Ba/Rb, Th/U, Nb/U) occur at

low degrees of partial melting (La/Sm $\sim$ 6, Fig. 9), which is coincident with the HREE starting to fractionate (Fig. 3, La/Sm vs Yb). On the other hand, the abrupt changes in other element ratios (e.g. Rb/Cs, Ce/Pb, Sr/Nd, Zr/Sm, Nb/Ta, H_2O/Ce) seem to happen at higher melt fractions (La/Sm $\sim$ 4–5). This points to the melting-out or breakdown of phases in the mantle source, so the relative incompatibility of many trace elements changes. Unfortunately, our limited isotope data are not sufficient to trace the origin of documented bends in element ratio trends (Figs 3 and 9).

In conclusion, rocks with isotope, and major and trace element compositions lying well within the compositional range of Macquarie Island glasses were recovered from DSDP Sites 279A (Macquarie Ridge north of Macquarie Island) and 274 (Balleny Basin southeast of the Balleny Islands; Pyle *et al.*, 1995). This supports our assumption that the mantle heterogeneity implicated in this study is not related directly to Balleny plume mantle or magmas, but is more likely to be a regional signature.

REFERENCES

Adamson, D. A., Selkirk, P. M., Price, D. M. & Selkirk, J. M. (1996). Pleistocene uplift and palaeoenvironments of Macquarie Island:

evidence from palaeobeaches and sedimentary deposits. *Papers and Proceedings of the Royal Society of Tasmania* **130**, 25–32.

Allan, J. F., Chase, R. L., Cousens, B., Michael, P. J., Gorton, M. P. & Scott, S. D. (1993). The Tuzo Wilson volcanic field, NE Pacific: alkaline volcanism at a complex, diffuse, transform–trench–ridge triple junction. *Journal of Geophysical Research* **98**, 22367–22387.

Allan, J. F., Batiza, R. & Sack, R. O. (1994). Geochemical characteristics of Cocos Plate seamount lavas. *Contributions to Mineralogy and Petrology* **116**, 47–61.

Basylev, B. A. & Kamenetsky, V. S. (1998). Genesis of peridotites from the ophiolite complex of Macquarie Island, southwestern Pacific Ocean. *Petrology* **6**, 335–350.

Batiza, R. & Vanko, D. (1984). Petrology of young Pacific seamounts. *Journal of Geophysical Research* **89**, 11235–11260.

Bougault, H., Dmitriev, L., Schilling, J. G., Sobolev, A., Joron, J. L. & Needham, H. D. (1988). Mantle heterogeneity from trace elements: MAR triple junction near 14°N. *Earth and Planetary Science Letters* **88**, 27–36.

Cande, S. C., Stock, J., Raymond. C. & Müller, R. D. (1998). New constraints on plate tectonic puzzle of the SW Pacific. *Eos Transactions, American Geophysical Union* **79**, 81–82.

Christodoulou, C., Griffin, B. J. & Foden, J. (1984). The geology of Macquarie Island. *ANARE Research Notes* **21**, 1–15.

Danyushevsky, L. V., Falloon, T. J., Sobolev, A. V., Crawford, A. J., Carroll, M. & Price, R. C. (1993). The H₂O content of basalt glasses from southwest Pacific back-arc basins. *Earth and Planetary Science Letters* **117**, 347–362.

Dick, H. J. B. (1989). Abyssal peridotites, very slow spreading ridges and ocean ridge magmatism. In: Saunders, A. D. & Norry, M. J. (eds) *Magmatism in the Ocean Basins. Geological Society, London, Special Publication* **42**, 71–105.

Duncan, R. A. & Varne, R. (1988). The age and distribution of the igneous rocks of Macquarie Island. *Papers and Proceedings of the Royal Society of Tasmania* **122**, 45–50.

Dupre, B., Lambert, B., Rousseau, D. & Allègre, C. J. (1981). Limitations on the scale of mantle heterogeneity under oceanic ridges. *Nature* **294**, 552–554.

Eggins, S. M. (1992). Petrogenesis of Hawaiian tholeiites: 2, aspects of dynamic melt segregation. *Contributions to Mineralogy and Petrology* **110**, 398–410.

Eggins, S. M., Rudnick, R. L. & McDonough, W. F. (1998). The composition of peridotites and their minerals: a laser-ablation ICP-MS study. *Earth and Planetary Science Letters* **154**, 53–71.

Ford, C. E., Russel, D. G., Graven, J. A. & Fisk, M. R. (1983). Olivine–liquid equilibria: temperature, pressure and composition dependence of the crystal/liquid cation partition coefficients for Mg, Fe²⁺, Ca and Mn. *Journal of Petrology* **24**, 256–265.

Frey, F. A., Walker, N., Stakes, D., Hart, S. R. & Nielsen, R. (1993). Geochemical characteristics of basaltic glasses from the AMAR and FAMOUS axial valleys, Mid-Atlantic Ridge (36°–37°N): petrogenetic implications. *Earth and Planetary Science Letters* **115**, 117–136.

Fujii, T. & Scarfe, C. M. (1985). Composition of liquids coexisting with spinel lherzolite at 10 kbar and the genesis of MORBs. *Contributions to Mineralogy and Petrology* **90**, 18–28.

Goscombe, B. D. & Everard, J. L. (1998). Geology of Macquarie Island, sheets 1–7. *Geological Atlas 1:10 000 series*. Rosny Park: Tasmanian Geological Survey.

Goscombe, B. D. & Everard, J. L. (1999). Macquarie Island mapping reveals three tectonic phases. *Eos Transactions, American Geophysical Union* **80**, 50.

Griffin, B. J. (1982). Igneous and metamorphic petrology of lavas and dykes of the Macquarie Island ophiolite complex. Ph.D. thesis, University of Tasmania, Hobart.

Griffin, B. J. & Varne, R. (1980). The Macquarie Island ophiolite complex: Mid-Tertiary oceanic lithosphere from a major ocean basin. *Chemical Geology* **30**, 285–308.

Hart, S. R. (1988). Heterogeneous mantle domains: signatures, genesis and mixing chronologies. *Earth and Planetary Science Letters* **90**, 273–296.

Hayes, D. E. & Talwani, M. (1972). Geophysical investigation of the Macquarie ridge complex. In: Hayes, D. E. (ed.) *Antarctic Oceanology II: The Australian–New Zealand Sector. Antarctic Research Series, American Geophysical Union* **19**, 211–234.

Hekinian, R., Thompson, G. & Bideau, D. (1989). Axial and off-axial heterogeneity of basaltic rocks from the East Pacific Rise at 12°35′–12°51′N. *Journal of Geophysical Research* **94**, 17437–17463.

Housh, T. B. & Luhr, J. F. (1991). Plagioclase–melt equilibria in hydrous system. *American Mineralogist* **76**, 477–492.

Jaques, A. L. & Green, D. H. (1980). Anhydrous melting of peridotite at 0–15 kb pressure and the genesis of tholeiitic basalts. *Contributions to Mineralogy and Petrology* **73**, 287–310.

Johnson, T. & Molnar, P. (1972). Focal mechanisms and plate tectonics of the southwest Pacific. *Journal of Geophysical Research* **77**, 5000–5032.

Jones, T. D. & McCue, K. F. (1988). The seismicity and tectonics of the Macquarie Ridge. *Papers and Proceedings of the Royal Society of Tasmania* **122**, 51–57.

Kamenetsky, V. (1996). Methodology for the study of melt inclusions in Cr-spinel, and implications for parental melts of MORB from FAMOUS area. *Earth and Planetary Science Letters* **142**, 479–486.

Kamenetsky, V. & Crawford, A. J. (1998). Melt–peridotite reaction recorded in the chemistry of spinel and melt inclusions in basalt from 43°N, Mid-Atlantic Ridge. *Earth and Planetary Science Letters* **164**, 345–352.

Kamenetsky, V. S., Eggins, S. M., Crawford, A. J., Green, D. H., Gasparon, M. & Falloon, T. J. (1998). Calcic melt inclusions in primitive olivine at 43°N MAR: evidence for melt–rock reaction/melting involving clinopyroxene-rich lithologies during MORB generation. *Earth and Planetary Science Letters* **160**, 115–132.

Kinzler, R. J. & Grove, T. L. (1992a). Primary magmas of mid-ocean ridge basalts 1. Experiments and methods. *Journal of Geophysical Research* **97**, 6885–6906.

Kinzler, R. J. & Grove, T. L. (1992b). Primary magmas of mid-ocean ridge basalts. 2. Applications. *Journal of Geophysical Research* **97**, 6907–6926.

Klein, E. M. & Langmuir, C. H. (1987). Global correlations of ocean ridge basalt chemistry with axial depth and crustal thickness. *Journal of Geophysical Research* **92**, 8089–8115.

Klein, E. M., Langmuir, C. H. & Staudigel, H. (1991). Geochemistry of basalts from the Southeast Indian Ridge, 115°E–138°E. *Journal of Geophysical Research* **96**, 2089–2107.

Lamarche, G., Collot, J.-Y., Wood, R. A., Sosson, M., Sutherland, R. & Delteil, J. (1997). The Oligocene–Miocene Pacific–Australia plate boundary, south of New Zealand: evolution from oceanic spreading to strike-slip faulting. *Earth and Planetary Science Letters* **148**, 129–139.

Langmuir, C. H., Bender, J. F., Bence, A. E., Hanson, G. N. & Taylor, S. R. (1977). Petrogenesis of basalts from the FAMOUS area: Mid-Atlantic Ridge. *Earth and Planetary Science Letters* **36**, 133–156.

Langmuir, C. H., Klein, E. M. & Plank, T. (1992). Petrological systematics of mid-ocean ridge basalts: constraints on melt generation beneath ocean ridges. In: Phipps Morgan, J., Blackman, D. K. & Sinton, J. M. (eds) *Mantle Flow and Melt Generation at Mid-ocean Ridges* **71**. Washington, DC: American Geophysical Union, pp. 183–280.

Lanyon, R. (1994). Mantle reservoirs and mafic magmatism associated with the break-up of Gondwana—the Balleny Plume and the Australian–Antarctic discordance. U–Pb zircon dating of a Proterozoic mafic dyke swarm in the Vestfold Hills, East Antarctica. Ph.D. thesis, University of Tasmania, Hobart.

Lanyon, R., Varne, R. & Crawford, A. J. (1993). Tasmanian Tertiary basalts, the Balleny plume, and opening of the Tasman Sea (southwest Pacific Ocean). *Geology* **21**, 555–558.

le Roex, A. P., Dick, H. J. B., Erlank, A. J., Reid, A. M., Frey, F. A. & Hart, S. R. (1983). Geochemistry, mineralogy and petrogenesis of lavas erupted along the southwest Indian Ridge between the Bouvet triple junction and 11 degrees east. *Journal of Petrology* **24**, 267–318.

le Roex, A., Dick, H. J. B. & Watkins, R. T. (1992). Petrogenesis of anomalous K-enriched MORB from the Southwest Indian Ridge: 11°53′E to 14°38′E. *Contributions to Mineralogy and Petrology* **110**, 253–268.

Lees, T. R. (1987). Report on geological observations, Macquarie Island, December 1986 to January 1987. Kingston, Tas.: Antarctic Division.

Longerich, H. P., Jackson, S. E. & Gunther, D. (1996). Laser ablation inductively coupled plasma mass spectrometric transient signal data acquisition and analyte concentration calculation. *Journal of Analytical Atomic Spectrometry* **11**, 899–904.

Maaloe, S. (1982). Geochemical aspects of permeability controlled partial melting and fractional crystallization. *Geochimica et Cosmochimica Acta* **46**, 43–57.

Macdougall, J. D. & Lugmair, G. W. (1986). Sr and Nd isotopes in basalts from the East Pacific Rise: significance for mantle heterogeneity. *Earth and Planetary Science Letters* **77**, 273–284.

Massell, C., Coffin, M. F., Mann, P., Frohlich, C., Schuur, C. L., Karner, G., Ramsay, D. & Lebrun, J.-F. (2000). Neotectonics of the Macquarie Ridge Complex, Australia–Pacific plate boundary. *Journal of Geophysical Research* in press.

Matveyenkov, V. V. & Baranov, B. V. (1981). Magmatic rocks of the Macquarie Ridge (southwest part of the Pacific Ocean). *International Geology Review* **23**, 417–425.

Maurel, C. & Maurel, P. (1982). Experimental study on Fe^{2+}–Fe^{3+} equilibria in chrome spinels and coexisting alkalic silicate liquids, at one atmosphere pressure. *Comptes Rendus de l'Académie des Sciences* **295**, 209–212.

Mawson, D. (1943). Macquarie island, its geography and geology. *Australasian Antarctic Expedition 1911–1914, Scientific Report Section A 5*. Sydney, N.S.W.: Government Printing Office.

McKenzie, D. & Bickle, M. J. (1988). The volume and composition of melt generated by extension of the lithosphere. *Journal of Petrology* **29**, 625–679.

Michael, P. J., Chase, R. L. & Allen, J. F. (1989). Petrologic and geologic variations along the southern Explorer Ridge, northeast Pacific Ocean. *Journal of Geophysical Research* **94**, 13895–13918.

Mortimer, N. (1995). Igneous and sedimentary rocks dredged from the northern Macquarie Ridge, Southern Ocean. *AGSO Journal of Australian Geology and Geophysics* **15**, 529–537.

Natland, J. H. (1989). Partial melting of a lithologically heterogeneous mantle: inferences from crystallization histories of magnesian abyssal tholeiites from the Siqueiros Fracture Zone. In: Saunders, A. D. & Norry, M. J. (eds) *Magmatism in the Ocean Basins. Geological Society, London, Special Publication* **42**, 41–70.

Niu, Y. & Batiza, R. (1997). Trace element evidence from seamounts for recycled oceanic crust in the Eastern Pacific mantle. *Earth and Planetary Science Letters* **148**, 471–484.

Niu, Y., Waggoner, D. G., Sinton, J. M. & Mahoney, J. J. (1996). Mantle source heterogeneity and melting processes beneath seafloor spreading centers: the East Pacific Rise, 18°–19°S. *Journal of Geophysical Research* **101**, 27711–27733.

Niu, Y., Collerson, K. D., Batiza, R., Wendt, J. I. & Regelous, M. (1999). Origin of enriched-type mid-ocean ridge basalt at ridges far from mantle plumes: the East Pacific Rise at 11°20′N. *Journal of Geophysical Research* **104**, 7067–7087.

Ovenshine, A. T., Winkler, G. R., Andrews, P. B. & Gostin, V. A. (1974). Chemical analyses and minor element composition of Leg 29 basalts. In: White, S. M. (ed.) *Initial Reports of the Deep Sea Drilling Project, 29*. Washington, DC: US Government Printing Office, pp. 1097–1102.

Plank, T. & Langmuir, C. H. (1992). Effects of the melting regime on the composition of the oceanic crust. *Journal of Geophysical Research* **97**, 19749–19770.

Pyle, D. G., Christie, D. M., Mahoney, J. J. & Duncan, R. A. (1995). Geochemistry and geochronology of ancient southeast Indian and southwest Pacific seafloor. *Journal of Geophysical Research* **100**, 22261–22282.

Quilty, P. G., Rubenach, M. & Wilcoxon, J. A. (1973). Miocene ooze from Macquarie Island. *Search* **4**, 163–164.

Ruff, L. J., Given, J. W., Sanders, S. O. & Sperber, C. M. (1989). Large earthquakes in the Macquarie Ridge complex: transitional tectonics and subduction initiation. *Pure and Applied Geophysics* **129**, 71–129.

Schilling, J.-G. & Ridley, W. I. (1974). Volcanic rocks from DSDP Leg 29: petrography and rare-earth abundances. In: White, S. M. (ed.) *Initial Reports of the Deep Sea Drilling Project, 29*. Washington: US Government Printing Office, pp. 1103–1107.

Schilling, J.-G., Kingsley, R. H. & Devine, J. D. (1982). Galapagos hot spot-spreading center system, I. Spatial petrological and geochemical variations, 83°W–101°W. *Journal of Geophysical Research* **87**, 5593–5610.

Schilling, J.-G., Zajac, M., Evans, R., Johnston, T., White, W., Devine, J. D. & Kingsley, R. (1983). Petrologic and geochemical variations along the Mid-Atlantic Ridge from 29°N to 73°N. *American Journal of Science* **283**, 510–586.

Shibata, T., Thompson, G. & Frey, F. A. (1979). Tholeiitic and alkali basalts from the Mid-Atlantic Ridge at 43°N. *Contributions to Mineralogy and Petrology* **70**, 127–141.

Shimizu, N. (1994). Depths of melting and melt extraction beneath mid-ocean ridges as recorded in melt inclusions. *Mineralogical Magazine* **58A**, 829–830.

Sobolev, A. V. & Shimizu, N. (1993). Ultra-depleted primary melt included in an olivine from the Mid-Atlantic Ridge. *Nature* **363**, 151–154.

Sobolev, A. V. & Shimizu, N. (1994). The origin of typical NMORB: the evidence from a melt inclusions study. *Mineralogical Magazine* **58A**, 862–863.

Stock, J. & Molnar, P. (1982). Uncertainties in the relative positions of the Australia, Antarctica, Lord Howe, and Pacific plates since the Late Cretaceous. *Journal of Geophysical Research* **B87**, 4697–4714.

Summerhayes, C. P. (1969). Marine geology of the New Zealand Subantarctic sea-floor. *New Zealand Department of Scientific and Industrial Research Bulletin* **190**, 1–90.

Sun, S.-S. & McDonough, W. F. (1989). Chemical and isotopic systematics of oceanic basalts: implications for mantle composition and processes. In: Saunders, A. D. & Norry, M. J. (eds) *Magmatism in the Ocean Basins. Geological Society, London, Special Publication* **42**, 313–345.

Sutherland, R. (1995). The Australia–Pacific boundary and Cenozoic plate motions in the SW Pacific: some constraints from Geosat data. *Tectonics* **14**, 819–831.

Tsamerian, O. P. & Sobolev, A. V. (1996). The evidence for extremely low degree of melting under Mid-Atlantic Ridge at 14°N. *V. M. Goldschmidt Conference*, p. 628.

Varne, R. (1989). Macquarie Island. In: Burrett, C. F. & Martin, E. L. (eds) *Geology and Mineral Resources of Tasmania. Special Publication, Geological Society of Australia* **15**, 398–402.

Varne, R. & Rubenach, M. J. (1972). Geology of Macquarie Island and its relationship to oceanic crust. In: Hayes, D. E. (ed.) *Antarctic Oceanology II: The Australian–New Zealand Sector. Antarctic Research Series, American Geophysical Union* **19**, 251–266.

Varne, R., Gee, R. D. & Quilty, P. G. J. (1969). Macquarie Island and the cause of oceanic linear magnetic anomalies. *Science* **166**, 230–233.

Varne, R., Brown, A. V., Jenner, G. A. & Falloon, T. (2000). Macquarie Island : its geology and structural history, and the timing and tectonic setting of its N-MORB to E-MORB magmatism. In: Dilek, Y., Moores, E. M., Elthon, D. & Nicolas, A. (eds) *Ophiolites and Oceanic Crust: New Insights from Field Studies and Ocean Drilling Program. Geological Society of America, Special Publication* in press.

Walcott, R. I. (1978). Present tectonics and Late Cenozoic evolution of New Zealand. *Geophysical Journal of the Royal Astronomical Society* **52**, 137–164.

Watkins, N. D. & Gunn, B. M. (1971). Petrology, geochemistry, and magnetic properties of some rocks dredged from the Macquarie ridge. *New Zealand Journal of Geology and Geophysics* **14**, 153–168.

Weaver, B. L. (1991). The origin of ocean island basalt end-member compositions: trace element and isotopic constraints. *Earth and Planetary Science Letters* **104**, 381–397.

Weissel, J. K., Hayes, D. E. & Herron, E.M. (1977). Plate tectonics synthesis: the displacements between Australia, New Zealand, and Antarctica since the late Cretaceous. *Marine Geology* **25**, 231–277.

Williamson, P. (1979). The paleomagnetism of outcropping oceanic crust on Macquarie Island. *Journal of the Geological Society of Australia* **25**, 387–394.

Williamson, P. E. (1988). Origin, structural and tectonic history of the Macquarie Island region. *Papers and Proceedings of the Royal Society of Tasmania* **122**, 27–43.

Williamson, P. & Johnson, B. D. (1974). Crustal structure of the central region of the Macquarie Ridge Complex from gravity studies. *Marine Geophysical Researches* **2**, 127–132.

Wood, D. A. (1979). A variably veined suboceanic upper mantle—genetic significance for mid-ocean ridge basalts from geochemical evidence. *Geology* **7**, 499–503.

Wood, R., Lamarche, G., Herzer, R., Delteil, J. & Davy, B. (1996). Paleogene seafloor spreading in the southeast Tasman Sea. *Tectonics* **15**, 966–975.

Woodhead, J. D. (1996). Extreme HIMU in oceanic setting: the geochemistry of Mangaia Island (Polynesia), and temporal evolution of the Cook–Austral hotspot. *Journal of Volcanology and Geothermal Research* **72**, 1–19.

Zindler, A. & Hart, S. (1986). Chemical geodynamics. *Annual Review of Earth and Planetary Sciences* **14**, 493–571.

Zindler, A., Staudigel, H. & Batiza, R. (1984). Isotope and trace element geochemistry of young Pacific seamounts: implications for the scale of upper mantle heterogeneity. *Earth and Planetary Science Letters* **70**, 175–195.